Scholarly Research Journal for Interdisciplinary Studies
Online ISSN 2278-8808, SJIF 2024 = 8.153
https://www.srjis.com/issues_data/246
Peer Reviewed & Refereed Journal, JAN-FEB 2025, Vol- 13/87

RADIATIVE UNSTEADY SQUEEZING FLOW BETWEEN TWO PARALLEL PLATES WITH CONVECTIVE BOUNDARY CONDITIONS

Dr. Sapnali. L. Patil, Sanket S Pande & Amruta V Birajdar

M. G. V's Arts, science and Commerce College Manmad. 423104, India

Email- sapnalipande12@gmail.com

Paper Received On: 20 JAN 2025

Peer Reviewed On: 24 FEB 2025

Published On: 01 MAR 2025

Abstract

In this paper, we investigate the nonlinear radiation effects in a time dependent two-dimensional flow of a nanofluid squeezed between two parallel disks with convective boundary conditions. Transportations of heat and mass are characterized through thermal radiation and chemical reaction. Suitable similarity variables lead to convert governing partial differential equations into system of ordinary differential equations. The numerical solution of the ordinary differential equations is carried out by a MATLAB routine bvp4c. Effect of sundry physical parameters such as Squeezing number, Radiation parameter, Hartman number, Prandlt number, Brownian motion parameter, thermophoresis parameter, Nusselt number and Sherwood number are analyzed through graphs for the velocity, temperature and concentration profiles for both suction and blowing cases. Physical quantities of curiosity such as skin friction local Sherwood number and local Nusselt number at both disks are estimated and elaborated. Besides, comparative table is also designed to validate our present outcomes with previous limiting study.

Keywords: *Squeezing flow, Parallel disks, nonlinear radiation effect, Robin boundary conditions etc.*

Nomenclature:

A	Suction/ Blowing parameter
B	Strength of magnetic filed
B_0	Strength of magnetic filed
Bi_1, Bi_2	Biot numbers
Nt	Thermophoretic parameter
Nb	Brownian motion parameter

Le	Lewis Number
a, H	Positive constants
k	Thermal conductivity
k^*	Mean absorption coefficient
D_T	Thermophoretic diffusion coefficient
D_B	Brownian motion coefficient
S	Squeeze number
Cfr	Skin friction coefficient
Nur	Nuseelt number
Shr	Sherwood number
$h(t)$	Distance between the two disks
Nu	Nusselt number
Pr	Prandlt Number
P	Pressure
r / z	Space coordinate
T	Temperature
C	Concentration
C_h	Concentration at the upper disk
C_w	Concentration at the lower disk
u, w	Velocity components
w_0	Suction/blowing velocity
T_h	Temperature at the upper disk
T_w	Temperature at the lower disk
T_m	Mean fluid temperature
M	Hartman number
Re_r	Reynolds number
C_p	Specific heat
f	Dimensionless stream function
q_w	Surface heat flux

q_r Radioactive heat flux

Rd Radiation parameter

σ^* Stefan –Boltzman constant

Green Number:

η Similarity variable

τ Heat capacity

α Thermal diffusivity

μ Dynamic Viscosity

σ Electric conductivity

ρ Density

θ Dimensionless Temperature

ϕ Dimensionless Concentration

υ Viscous diffusivity

Introduction:

The term Squeezing flow is generated by natural stress or vertical velocities of the moving boundary layer. Recently the keen interest are found in the analysis of squeezed following to its prompt improvement in fluid dynamics and its implication in numerous practical and industrial utilizations like polymer processing, bio fluid mechanics like pumping of heart, food/chemical engineering, liquid-metal lubrication and power transmission. An approximasion on squeezing flow with lubrication was pioneer work done by Stefan [1]. Several attempts are reported that extended the traditional problem to heat transfer case. Fluid inertia characteristics in squeezed films are elaborated by Kuzma [2]. Siddiqui et al. [3] modeled transient MHD squeezed flow via channel. Analysis of magneto squeezed flow by infinite channel is described by Sweet et al. [4]. Different studies are available in literature that used various solution schemes to get analytical and numerical solutions for the said problem. Siddiqui et al. [5] examined two-dimensional MHD squeezing flow between parallel plates. For parallel disk similar problem has been discussed by Domairry and Aziz [6]. Both used Homotopy perturbation method (HPM) to determine the solution. Joneidi et al. [7] studied the mass transfer effect on squeezing flow between parallel

disks using Homotopy analysis method (HAM). Most recently influence of heat transfer in the MHD squeezing Flow between parallel disks has been investigated by T. Hayat et al. [8].

The investigations dealing with heat transport phenomenon are important in many industrial applications such as glass sheet productions, glass fiber, paper manufacturing, glass blowing, metal spinning, hot rolling, wire coating, the aerodynamic extrusion of plastic sheets, the continuous casting and the drawing of plastic films. The quality of the final product depends on the rate of heat transfer in various engineering and industrial processes involving high temperatures. Especially, the radiative effects have essence in controlling heat transfer rate in the cases where convective heat transfer coefficients are small and, in the polymer processing industry, the entire system involving the polymer extrusion process is placed in a thermally controlled environment. Moreover, the phenomenon of radiative heat transfer is essential in manufacturing industries for the design of reliable equipments, nuclear plants, gas turbines, various propulsion devices for aircraft, missiles, satellites and space vehicles. Also, the effects of thermal radiation in the forced and free convection flows are important in the space technology and processes occurring at high temperatures. Based on these applications, various researchers are engaged in studying different research problems dealing with the heat transport phenomenon when thermal radiation effects are present. For example, Cortell [9] presented the suction, viscous dissipation and thermal radiation effects in the flow of power law fluid past an infinite porous plate. Pal and Chatterjee [10] studied the heat and mass transfer effects in MHD non-Darcian flow of a micropolar fluid over a stretching sheet embedded in a porous media with non-uniform heat source and thermal radiations. Badruddin et al. [11] have numerically analyzed natural convection with thermal radiation inside a Darcy porous cavity using local thermal non-equilibrium model. Badruddin et al. [12] have studied numerically the combined effect of thermal radiation and viscous dissipation on natural convection in a Darcy porous vertical annular cylinder. Ahmed et al. [13] have studied MHD natural convection in a square differentially heated porous cavity taking into account the influence of viscous dissipation and radiation. Ahmed et al. [14] on the basis of the finite volume method have investigated natural convection and thermal radiation in an inclined porous cavity with corner heater. Mahapatra et al. [15] have analyzed the combined effects of thermal radiation and heat generation on free convection in a differentially heated square porous cavity. Umavathi et al. [16] analyzed that the Effect of thermal radiation on natural convection in a square porous cavity filled with a fluid of

temperature dependent viscosity. Analysis of radiated squeezed non-Newtonian (Eyring–Powell) material chemically reacted flow is scrutinized by Adesanya et al. [17] and Balazadeh et al. [18]. Effects of chemical reaction and thermal radiation on heat and mass transfer flow of MHD micropolar fluid in a rotating frame of reference has been investigated by Das [19]. Hayat et al. [20] studied the effects of thermal radiation in the flow of second grade fluid. Recently Bhattacharyya et al. [21] analyzed the effects of thermal radiation in micropolar fluid flow and heat transfer over a porous shrinking sheet.

The purpose of the current investigation is to analyze the thermal radiation effects when the flow is generated by squeezing of parallel disks with the convective boundary conditions. To our knowledge, very scarce literature deals with the thermal radiation effects in the axisymmetric flow geometries with robin boundary conditions. More precisely, we have extended the work of ref. [21] for the thermal radiation effect. Tables and graphical results are presented to analyze the flow.

Mathematical analysis:

Two-dimensional unsteady Squeezing flow of a nanoliquid between two parallel disks in the presence of magnetic field is addressed. The two parallel dicks are separated by a distance $h(t) = H(1-at)^{1/2}$. A magnetic field of strength $B(t) = B_0(1-at)^{-1/2}$ is applied perpendicular to the disks (see [7]) for physical configuration and coordinate system). Energy and concentration expressions accounted the terms radiation and first-order chemical reaction. Here T_w and C_w denotes the temperature and nanoparticles concentration at the lower disk while the temperature and concentration at upper disk are T_h and C_h respectively. The upper disk at $z = h(t)$ moves towards or away from the stationary lower disk with the velocity dh/dt. The flow configuration of present system is interpreted in Fig. 1. And the governing basic expressions for flow can be written as,

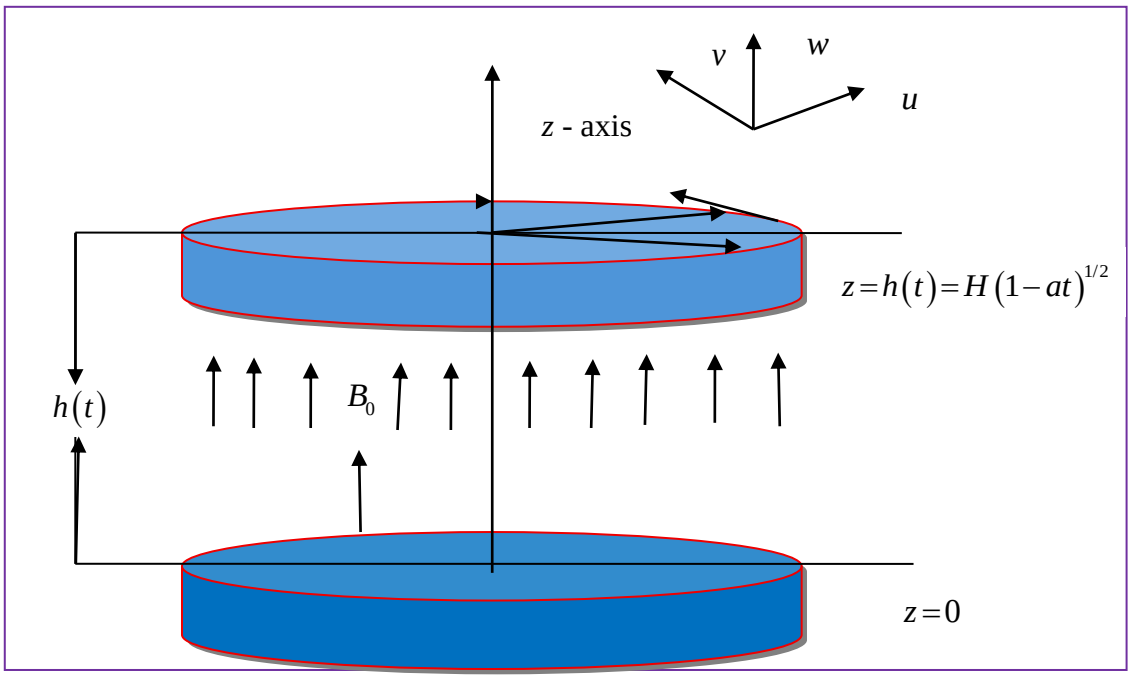

$$\frac{\partial u}{\partial r} + \frac{u}{r} + \frac{\partial w}{\partial r} = 0$$

(1)

$$\frac{\partial u}{\partial t} + u\frac{\partial u}{\partial r} + w\frac{\partial u}{\partial z} = \frac{-1}{\rho}\frac{\partial P}{\partial r} + \upsilon\left[\frac{\partial^2 u}{\partial r^2} + \frac{\partial^2 u}{\partial z^2} + \frac{1}{r}\frac{\partial u}{\partial r} - \frac{u}{r^2}\right] - \frac{\sigma}{\rho}B^2(t)u$$

(2)

$$\frac{\partial w}{\partial t} + u\frac{\partial w}{\partial r} + w\frac{\partial w}{\partial z} = \frac{-1}{\rho}\frac{\partial P}{\partial z} + \upsilon\left[\frac{\partial^2 w}{\partial r^2} + \frac{\partial^2 w}{\partial z^2} + \frac{1}{r}\frac{\partial w}{\partial r}\right]$$

(3)

$$\frac{\partial T}{\partial t} + u\frac{\partial T}{\partial r} + w\frac{\partial T}{\partial z} = \alpha\left[\frac{\partial^2 T}{\partial r^2} + \frac{1}{r}\frac{\partial T}{\partial r} + \frac{\partial^2 T}{\partial z^2}\right] + \tau\left[D_B\left(\frac{\partial C}{\partial r}\frac{\partial T}{\partial r} + \frac{\partial C}{\partial z}\frac{\partial T}{\partial z}\right) + \frac{D_T}{T_m}\left(\left(\frac{\partial T}{\partial r}\right)^2 + \left(\frac{\partial T}{\partial z}\right)^2\right)\right] - \frac{1}{\rho C_p}\frac{\partial q_r}{\partial z}$$

(4)

$$\frac{\partial C}{\partial t} + u\frac{\partial C}{\partial r} + w\frac{\partial C}{\partial z} = D_B\left[\frac{\partial^2 C}{\partial r^2} + \frac{1}{r}\frac{\partial C}{\partial r} + \frac{\partial^2 C}{\partial z^2}\right] + \frac{D_T}{T_m}\left[\frac{\partial^2 T}{\partial r^2} + \frac{1}{r}\frac{\partial T}{\partial r} + \frac{\partial^2 T}{\partial z^2}\right]$$

(5)

With the boundary conditions are

$$u = 0, w = \frac{dh}{dt}, -k\frac{\partial T}{\partial z}\bigg|_{z=h(t)} = h_2\left[T\left(r, z(t)\right) - T_h\right],\ C = C_h \qquad \text{at } z = h(t)$$

(6)

$$u = 0,\ w = \frac{-w_0}{\sqrt{1-at}}, -k\frac{\partial T}{\partial z}\bigg|_{z=0} = h_1\left[T_w - T(r,0)\right],\ C = C_w \qquad \text{at } z = 0$$

Here (u, w)- velocity components in the (r, z) directions respectively, ρ is the density, υ is the dynamic viscosity, σ is the electric conductivity , p is the pressure, T is the temperature, C is the concentration, α is the thermal diffusivity, D_B is the Brownian motion coefficient, D_T is the thermal diffusion coefficient, T_m is the mean fluid temperature and k is the thermal conductivity. The last term in the energy equation is the total diffusion mass flux for nanoparticles, given as a sum of two diffusion terms (Brownian motion and thermophoresis). Further τ is the dimensionless parameter that gives the ratio of effective heat capacity of the nanoparticles material to heat capacity of the fluid. Thus value of τ will be, therefore, different for different fluids and nanoparticles materials. Through Rosseland's approximation [23], the radioactive heat flux q_r is,

$$q_r = \frac{-4\sigma^*}{3k^*}\frac{\partial T^4}{\partial z},$$

(7)

Where k^* designates the coefficient of mean absorption and σ^* presents the Stefan-Boltzmann. Then consider $T^4 \cong -3T_h^4 + 4T_h^3 T$,

(8)

We have the equation from Eq. (7)

$$\frac{\partial q_r}{\partial z} = \frac{-16\sigma^* T_h^3}{3k^*}\frac{\partial^2 T}{\partial z^2}$$

(9)

Also we get, the energy equation can be converted in to flowing form,

$$\frac{\partial T}{\partial t} + u\frac{\partial T}{\partial r} + w\frac{\partial T}{\partial z} = \alpha\left[\frac{\partial^2 T}{\partial r^2} + \frac{1}{r}\frac{\partial T}{\partial r} + \frac{\partial^2 T}{\partial z^2}\right] + \tau\left[D_B\left(\frac{\partial C}{\partial r}\frac{\partial T}{\partial r} + \frac{\partial C}{\partial z}\frac{\partial T}{\partial z}\right) + \frac{D_T}{T_m}\left(\left(\frac{\partial T}{\partial r}\right)^2 + \left(\frac{\partial T}{\partial z}\right)^2\right)\right] + \frac{1}{\rho C_p}\frac{16\sigma^* T_h^3}{3k^*}\frac{\partial^2 T}{\partial z^2}$$

(10)

The non-dimensional variables can be defined as:

$$u = \frac{ar}{2(1-at)} f^{1}(\eta),\ \ w = \frac{aH}{\sqrt{1-at}} f(\eta),\ \eta = \frac{z}{H\sqrt{1-at}},$$

$$B(t) = \frac{B_0}{\sqrt{1-at}},\ \theta = \frac{T-T_h}{T_w-T_h},\ \ \phi = \frac{C-C_h}{C_w-C_h}$$

(11)

Then after eliminating pressure gradient expressions (2)- (5) and (10) gives to

$$f''' - S\left(\eta f''' + 3f'' - 2ff'''\right) - M^2 f'' = 0$$

(12)

$$\theta''\left[1+\frac{4}{3}Rd\right] + \Pr S\left(2f\theta' - \eta\theta'\right) + \Pr Nb\theta'\phi' + \Pr Nt\theta'^2 = 0$$

(13)

$$\phi'' + LeS\left(2f\phi' - \eta\phi'\right) + \frac{Nt}{Nb}\theta'' = 0$$

(14)

With the associated boundary conditions

$$f(0) = A,\ f'(0) = 0,\ \theta'(0) = Bi_1\left[\theta(0)-1\right],\ \phi(0) = 1$$

(15)

$$f(1) = \frac{1}{2},\ f'(1) = 0,\ \theta'(1) = Bi_1\left[\theta(1)\right],\ \phi(1) = 0$$

Where

$$A = \frac{w_0}{aH},\ S = \frac{aH^2}{2\upsilon},\ M = \sqrt{\frac{\sigma B_0^2 H^2}{\upsilon}},\ \Pr = \frac{\upsilon}{\alpha},\ Le = \frac{\upsilon}{D_e},$$

$$Nb = \frac{(\rho C)_p D_B (C_w - C_h)}{(\rho C)_f \upsilon},\ Nt = \frac{(\rho C)_p D_T (T_w - T_h)}{(\rho C)_f T_m \upsilon},\ Rd = \frac{4\sigma^* T_\infty^3}{kk^*}$$

(16)

The physical quantities of interest are skin friction coefficient C_{fr}, reduced Nusselt number Nur and reduced Sherwood number Shr are defined as

$$C_{fr} = \frac{\tau_{rz}\big|_{z=h(t)}}{\rho\left(\frac{-aH}{2(1-at)^{1/2}}\right)^2},\ Nur = \frac{H(q_w + q_r)}{k(T_w - T_h)},\ Shr = \frac{H\ j_w}{D_B(C_w - C_h)}$$

(17)

Where, $\tau_{rz} = \mu\left(\frac{\partial u}{\partial z} + \frac{\partial w}{\partial r}\right)\Big|_{z=h(t)}$, $q_w = -k\left(\frac{\partial T}{\partial z}\right)\Big|_{z=h(t)}$, $j_w = -D_B\left(\frac{\partial C}{\partial z}\right)\Big|_{z=h(t)}$

(18)

In terms of variables (6) we get

$$\frac{H^2}{r^2}\mathrm{Re}_r\, C_{fr} = f''(1),$$

$$Nur = (1-at)^{1/2}\, Nu = -\theta'(1)\,(1+\frac{4}{3}Rd),\ \ Shr = (1-at)^{1/2}\, Sh = -\phi'(1)$$

(19)

where $\mathrm{Re}_r = \frac{r\,a\,H(1-at)^{1/2}}{2\,\upsilon}$

(20)

Numerical Method:

The momentum, heat and mass transfer properties of nanofluid in a parallel disk with Soret and Dufour effects have not been studied yet because of the complexity of the system of governing equations. The governing system is highly nonlinear consisting of coupled ordinary differential equations that are quite difficult to solve analytically. Moreover, the presence of third kind boundary conditions makes the system more complicated. To overcome this deficiency, the system is numerically solved by a MATLAB routine based on a numerical method bvp4c offered by Kierzenka and Shampine [24]. Many engineering problems have been successfully solved by this method.

Results and Discussion:

Here we manifest in this section that how influential variables influences the non-dimensional velocity, temperature and concentration. To analyze the impact of such emerging parameters on the velocity, temperature and concentration profiles for suction $A > 0$ and blowing $A < 0$ with equal and unequal Biot numbers, effects of squeezing parameter S on the velocity and temperature profile are discussed in Figs. 2a and b. In the Figs 2a and 2b, we observed that the less velocity distribution is perceive for large values of

Squeezing parameter and behavior of squeeze number on velocity profile is opposite in blowing case as compared to suction case for both equal and unequal Biot numbers. Figures 3a and b signifies that effect of Hartman number on the velocity profiles. The velocity increases initially with an increase in M near the disks while in the center; velocity is decreases for both the cases as for equal and unequal Biot numbers. Also we observed that the effect of Hartman number M near the upper disk is more prominent as compared to the lower disk for both equal and unequal Biot numbers.

Figures 4a and b depicts the effect of Brownian motion parameter Nb on the temperature profile. It is evident that increasing the values of Brownian motion parameter Nb, effect of temperature profile is rises and move closer to the upper disk as for both suction and blowing cases with equal and unequal Biot numbers. Generally, Brownian motion helps to heat the fluid in the boundary layer and instantaneously impair particle deposition away from the fluid on the surface. Also the effect of thermophoresis parameter Nt on the temperature field for both the cases as equal and unequal Biot numbers are depicted in the Figs 5a and b. it is observed that increasing the values of thermophoresis parameter Nt enhance the temperature filed for both suction as well as for blowing cases with equal and unequal Biot numbers.

Also the effect of theses Brownian Motion parameter Nb and thermophoresis parameter Nt on the nanopartical volume fraction depicted in the Figs. 6a, b and 7a, b respectively for both equal and unequal Biot numbers. Increases the nanoparticle concentration with increasing the Brownian motion parameter Nb this is due to the effective movement of nanoparticles from the upper disk to the fluid. We also observe that the changes in the profiles only occur for the values of Nb in the range 0 to 2. Also there is increase in the concentration field as increasing the thermophoresis parameter for the both equal and unequal Biot numbers.

Variation in velocity, temperature and concentration for varying is depicted in Figs 8a, b, 9a, b and 10a, b for both equal and unequal Biot numbers. The Prandlt number $\Pr$ effect is less on the velocity is not much as compare to the temperature and concentration for suction and blowing case with both equal and unequal Biot numbers. As $\Pr$ increases the temperature profile is increase for $A<0$ and decreases for $A>0$ both the equal and unequal Biot numbers. The influence of Prandlt number $\Pr$ on the concentration field is displayed in the Figs. 10a and 10b for both equal and unequal Biot numbers. It shows that the increasing

the Prandlt number $\Pr$ the concentration field is decreases in blowing case and increases in suction case for both equal Biot number and for unequal Biot number. An argumentation in Rd is shows in Figs 11a b to 13a, b with respect to the velocity, temperature and concentration fields. The effect of Rd radiation parameter on velocity and concentration is very less for both suction and blowing cases with the equal and unequal Biot numbers. But the effect on the temperature filed, is decreases at the $A<0$ and increase at the $A>0$ for both equal and unequal Biot number.

In Figs 14a, b and 15a, b displayed that the combined influence of Brownian motion Nb and the thermophoresis parameters Nt on the reduced Nusselt number Nur and the Sherwood Numbers Shr for equal and unequal Biot numbers. Increasing the values of Brownian motion parameter Nb for weaker thermophoretic effect, there is slight increase in the magnitude of Nusselt number Nur for both equal and unequal Biot numbers. However increasing the values of Brownian motion parameter Nb and thermophoresis parameter Nt there is slight decrease in the magnitude of Sherwood number for both equal and unequal Biot numbers.

In the Table 1. shows the comparison of the present results with the Homotopy Analysis Method (HAM) for the velocity profile which discussed by the M. M. Hashmi et al. [25] for fixing the different squeezing parameter S and Hartman number M parameters. For fixed values of S and M , increase in the suction/blowing velocity corresponding to a larger rate of stress at the upper disk. The value of Skin friction coefficient decreases as the disk moves in the upward direction. Also increase in the magnetic field strength increases the Skin friction for both equal and unequal Biot numbers.

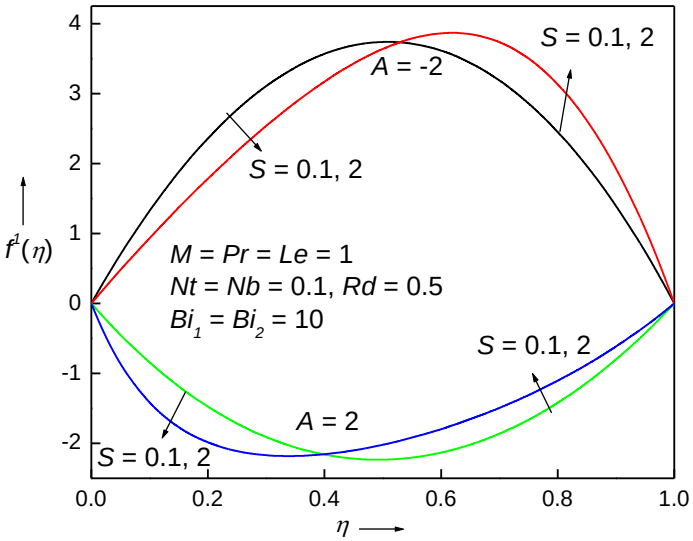

Fig. 2a Influence of S on $f^{1}(\eta)$ for equal Biot numbers

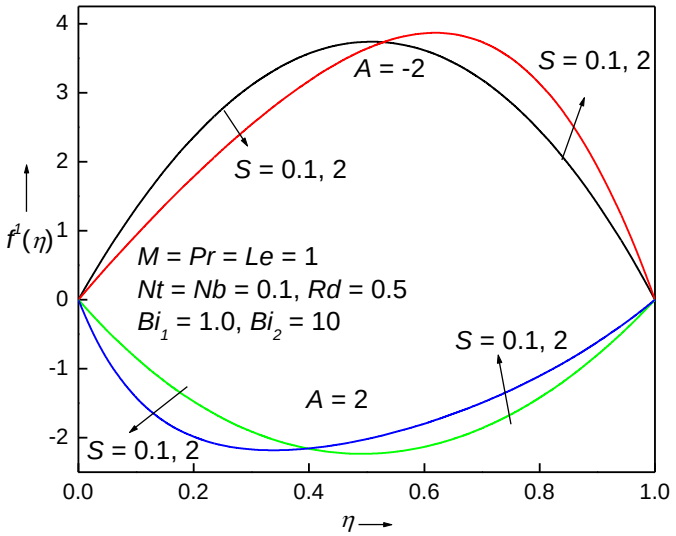

Fig 2b Influence of S on $f^{1}(\eta)$ for unequal Biot numbers

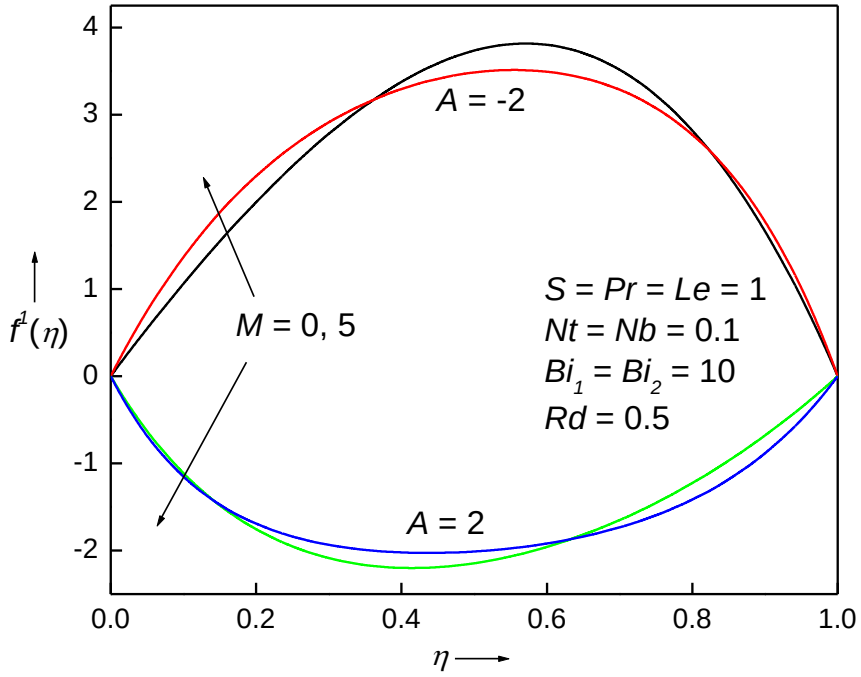

Fig 3a Influence of M on $f^1(\eta)$ for equal Biot numbers

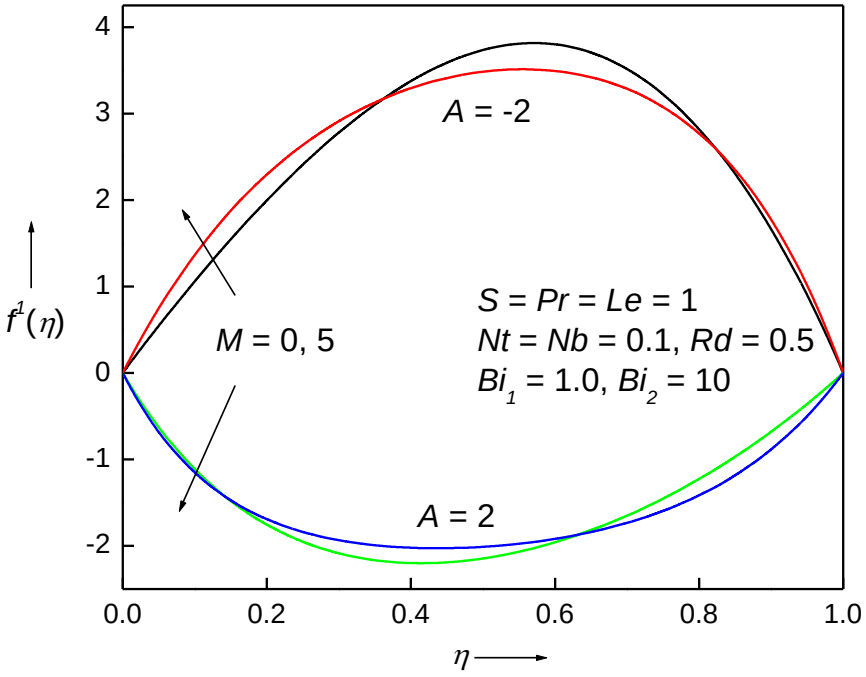

Fig 3b Influence of M on $f^1(\eta)$ for unequal Biot numbers

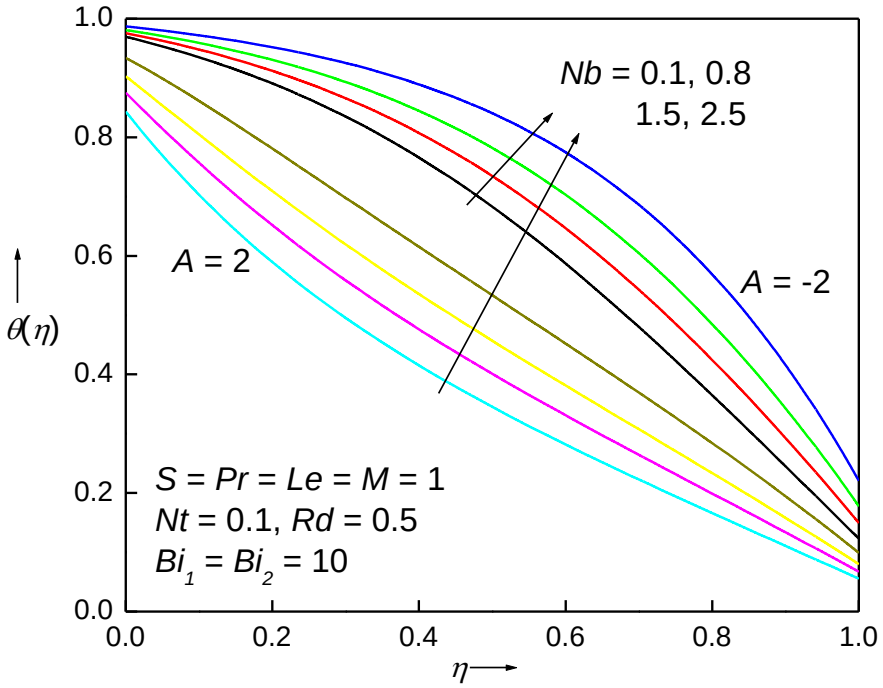

Fig 4a Influence of *Nb* on $\theta(\eta)$ for equal Biot numbers

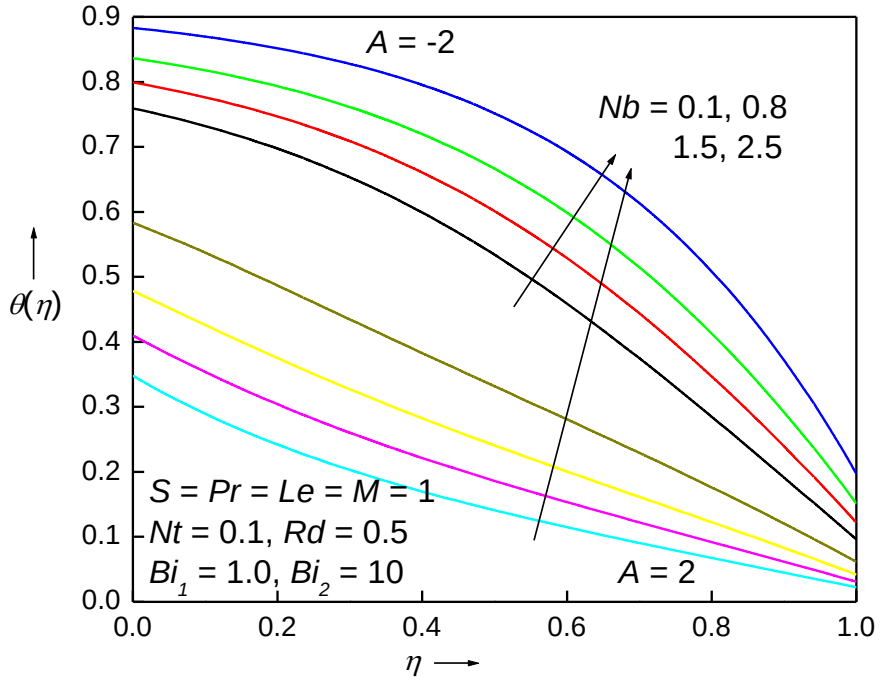

Fig 4b Influence of *Nb* on $\theta(\eta)$ for unequal Biot numbers

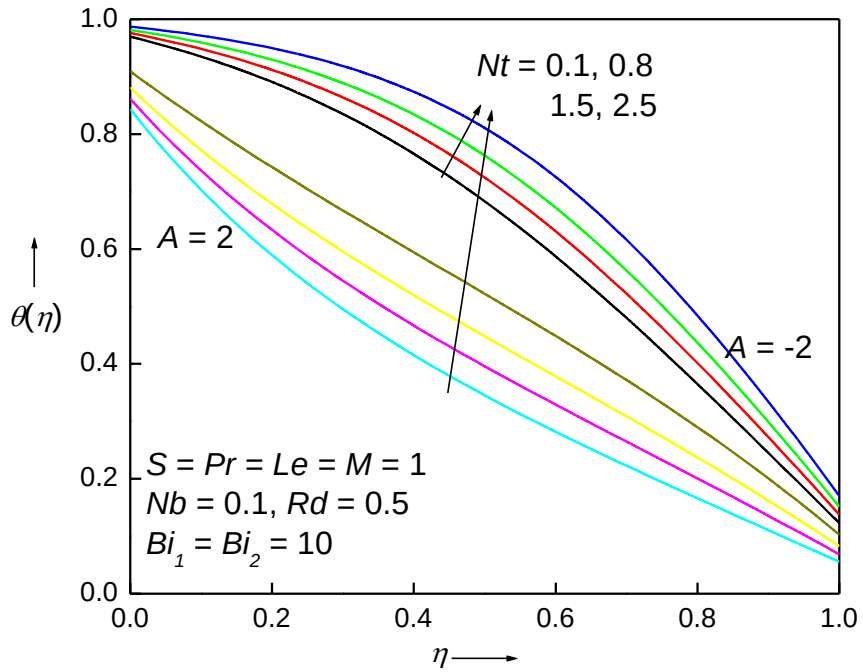

Fig 5a Influence of *Nt* on $\theta(\eta)$ for equal Biot numbers

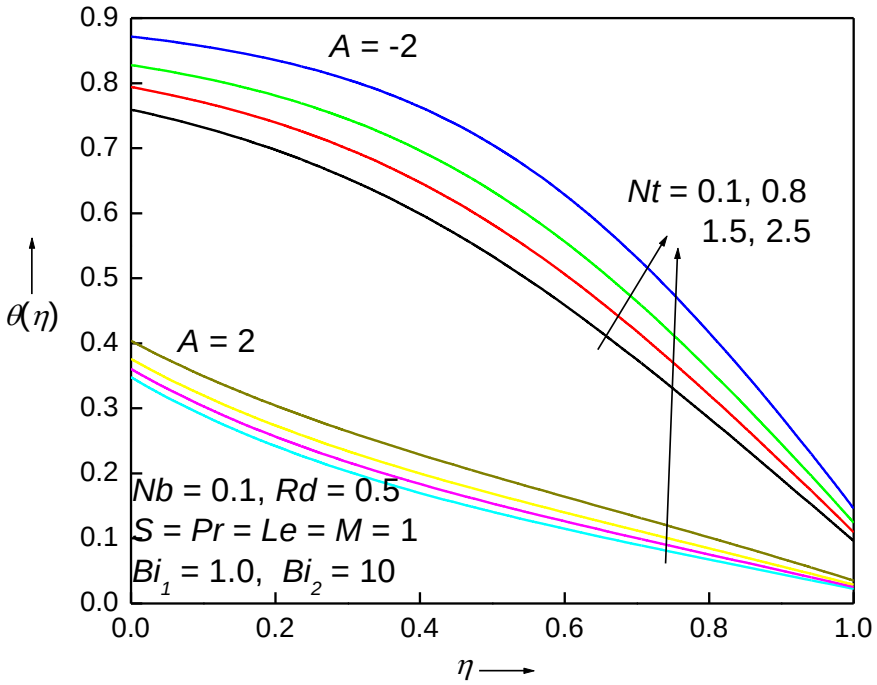

Fig 5b Influence of *Nt* on $\theta(\eta)$ for unequal Biot numbers

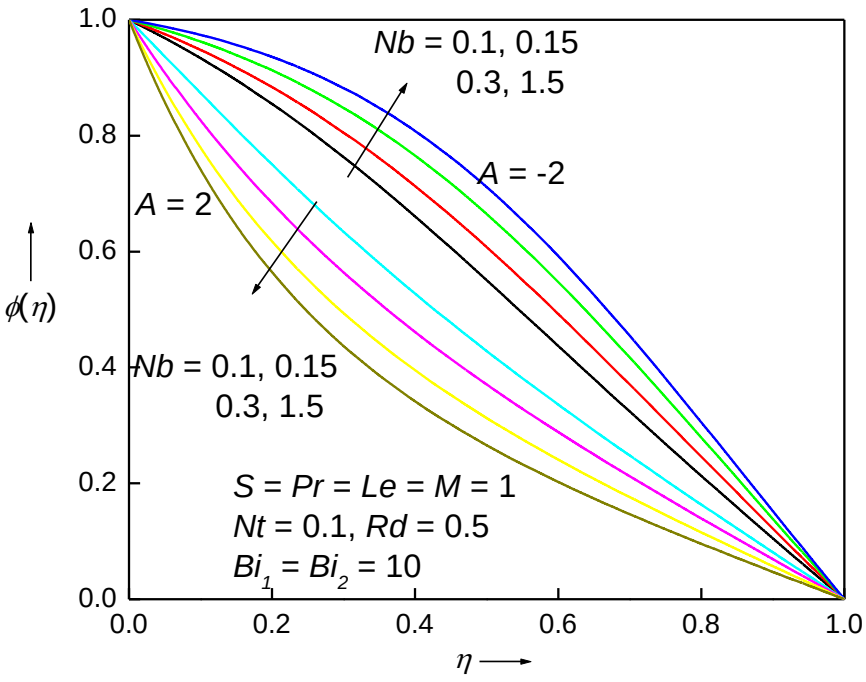

Fig 6a Influence of *Nb* on $\phi(\eta)$ for equal Biot numbers

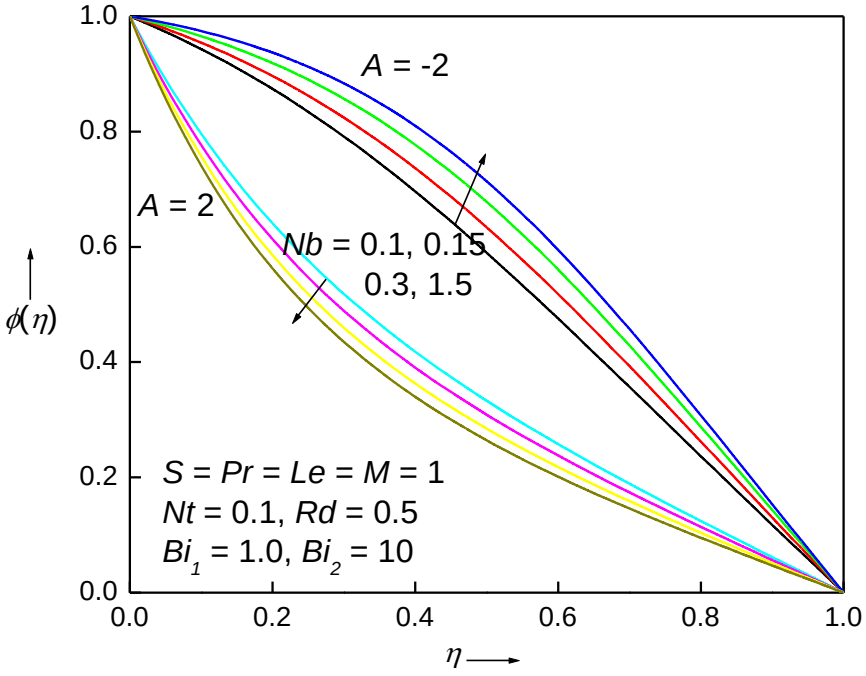

Fig 6b Influence of *Nb* on $\phi(\eta)$ for unequal Biot numbers

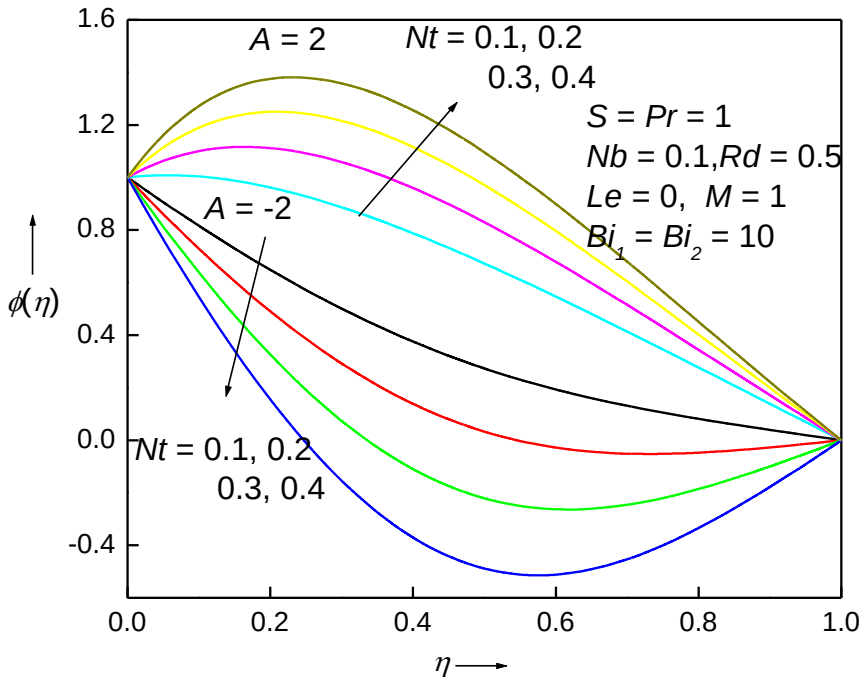

Fig 7a Influence of *Nt* on $\phi(\eta)$ for equal Biot numbers

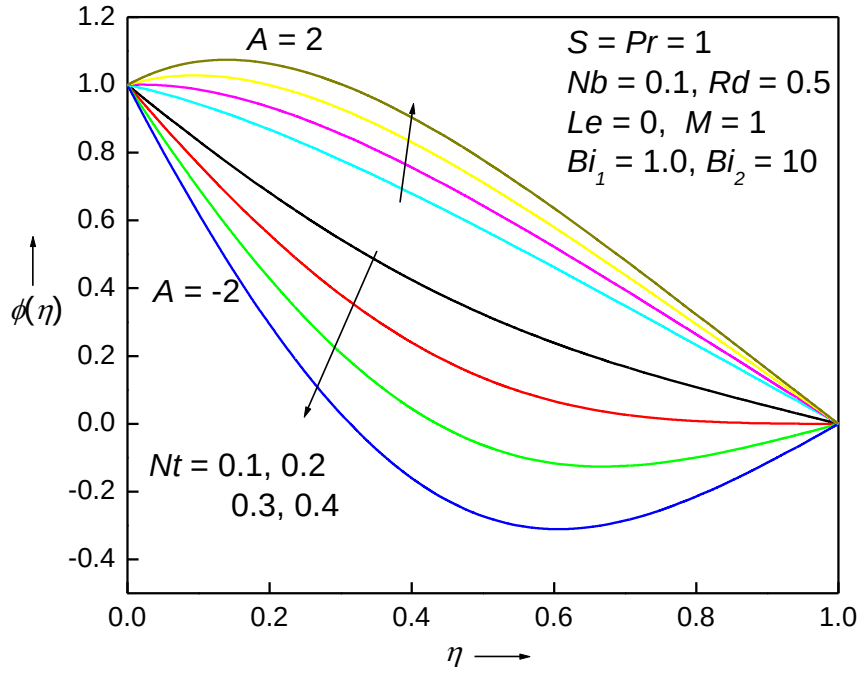

Fig 7b Influence of *Nt* on $\phi(\eta)$ for unequal Biot numbers

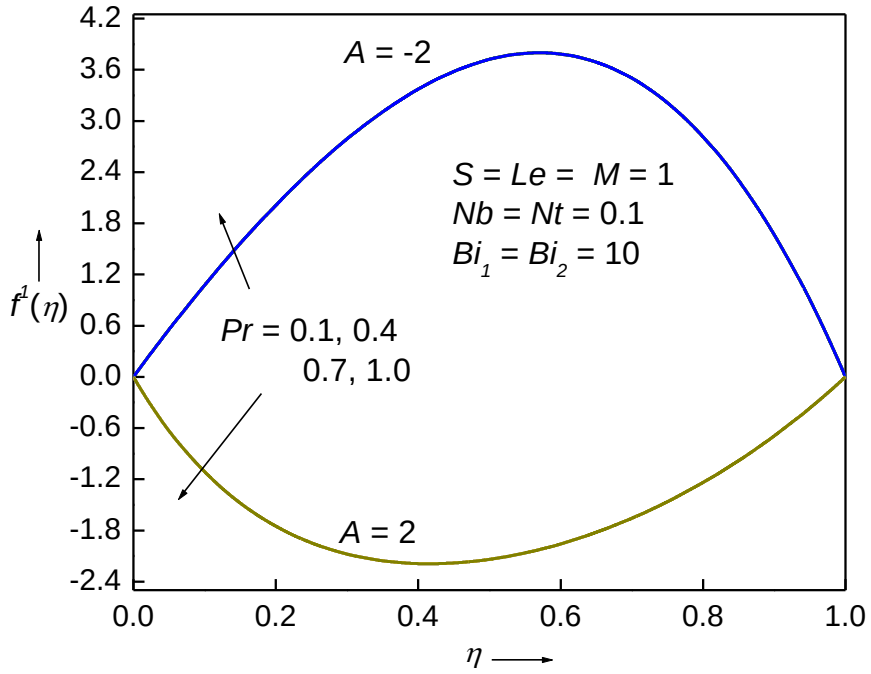

Fig 8a Influence of *Pr* on $f^{1}(\eta)$ for equal Biot numbers

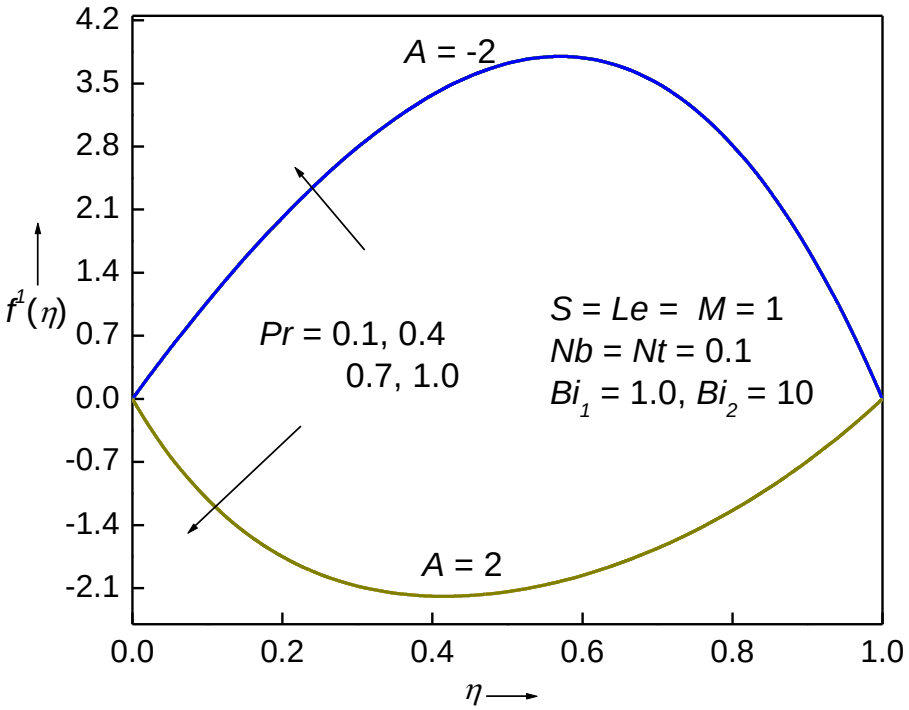

Fig 8b Influence of *Pr* on $f^{1}(\eta)$ for unequal Biot numbers

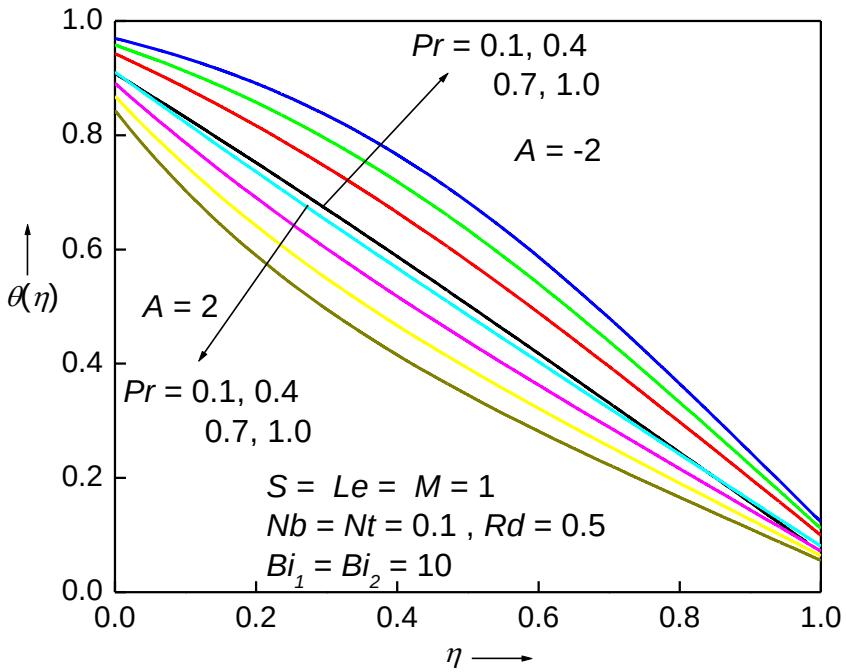

Fig 9a Influence of *Pr* on $\theta(\eta)$ for equal Biot numbers

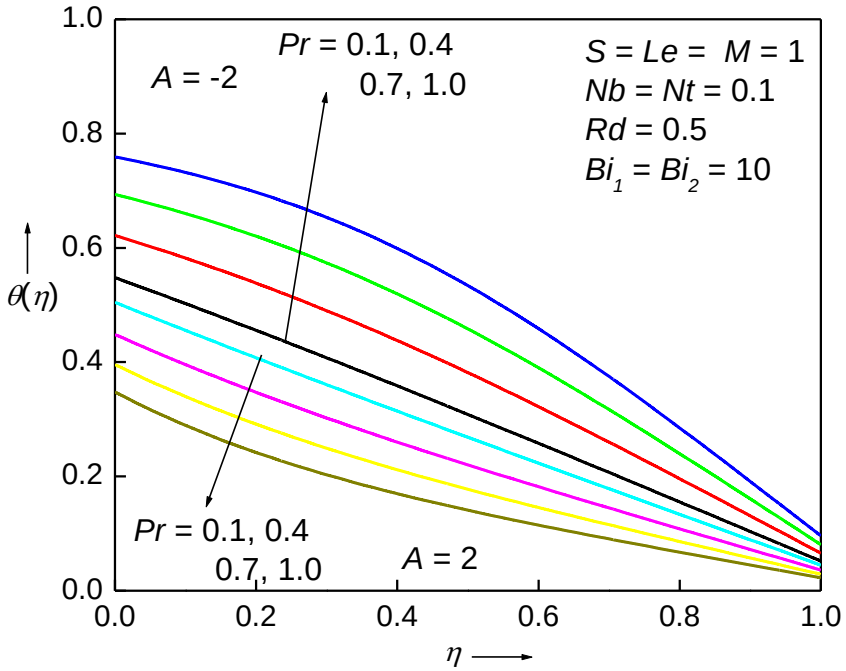

Fig 9b Influence of *Pr* on $\theta(\eta)$ for unequal Biot numbers

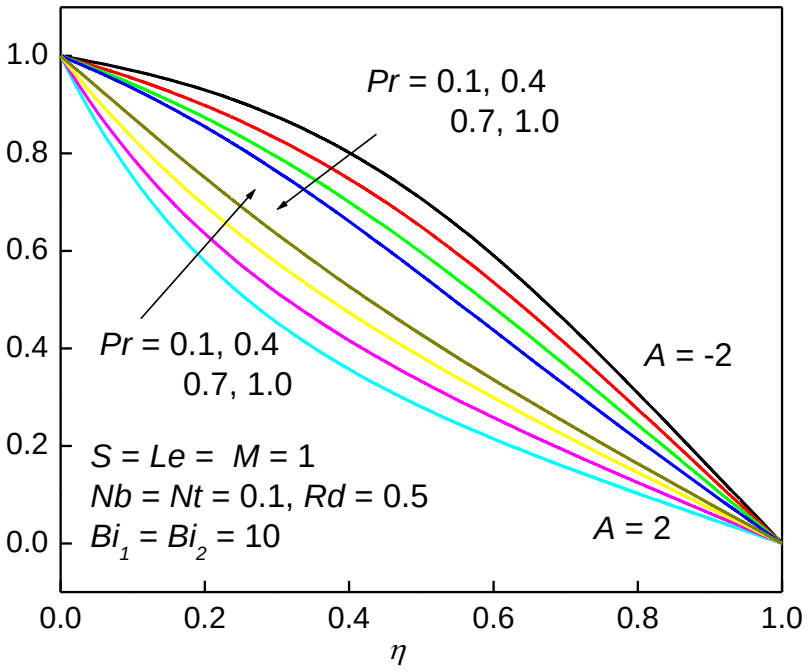

Fig 10a Influence of *Pr* on $\phi(\eta)$ for equal Biot numbers

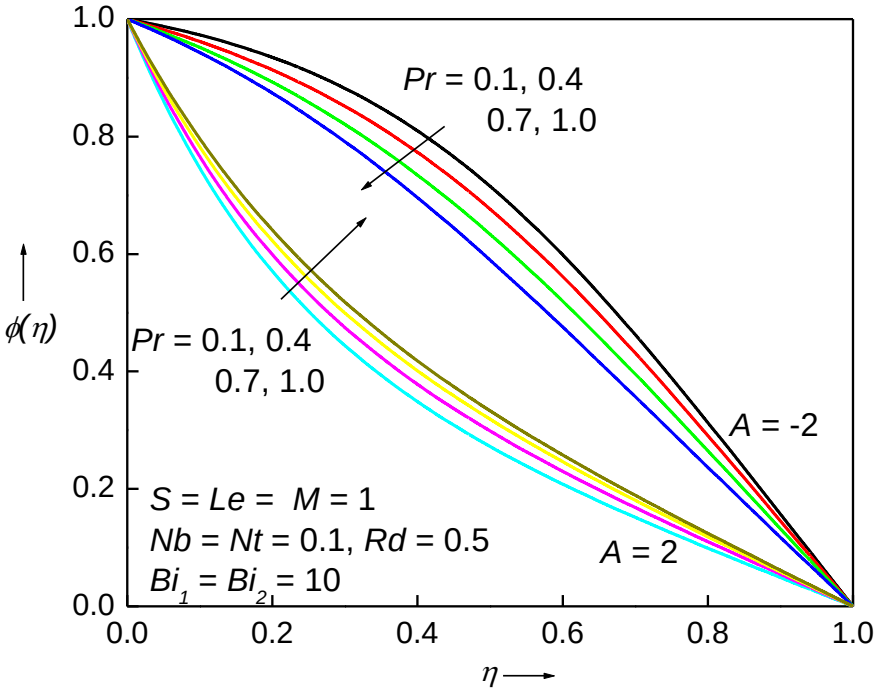

Fig 10b Influence of *Pr* on $\phi(\eta)$ for unequal Biot numbers

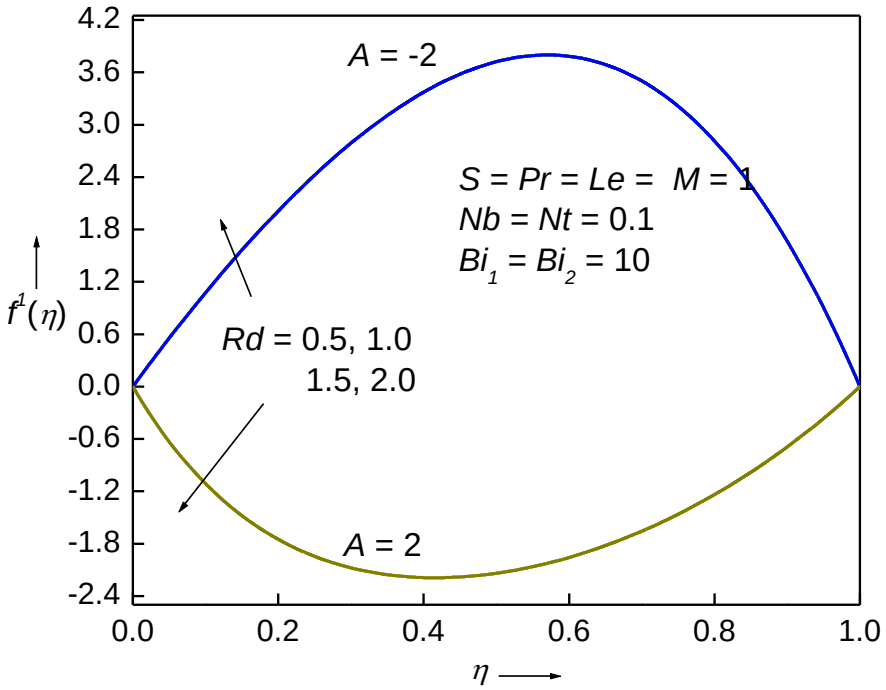

Fig 11a Influence of *Rd* on $f^1(\eta)$ for equal Biot numbers

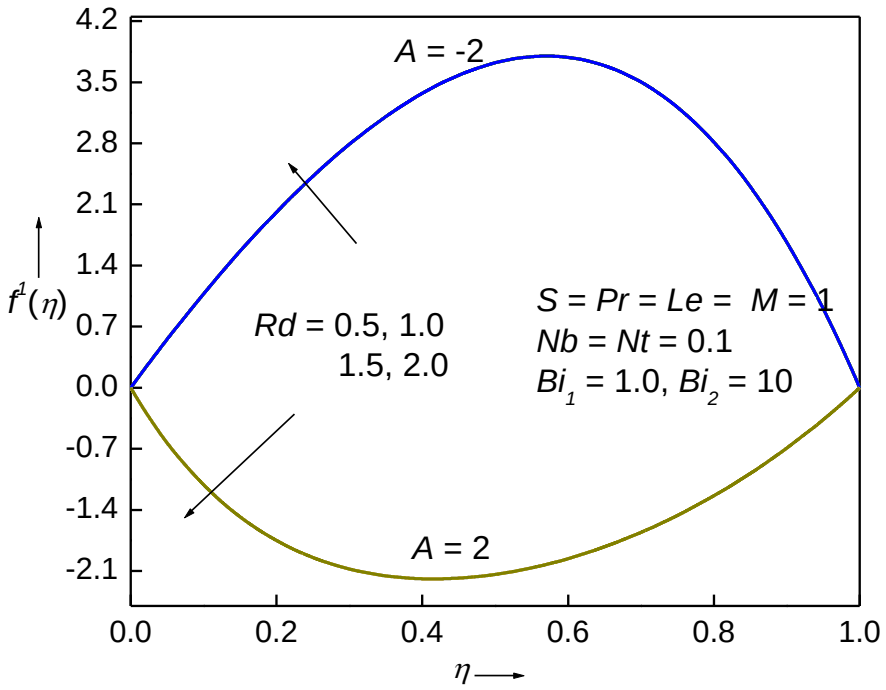

Fig 11b Influence of *Rd* on $f^1(\eta)$ for unequal Biot numbers

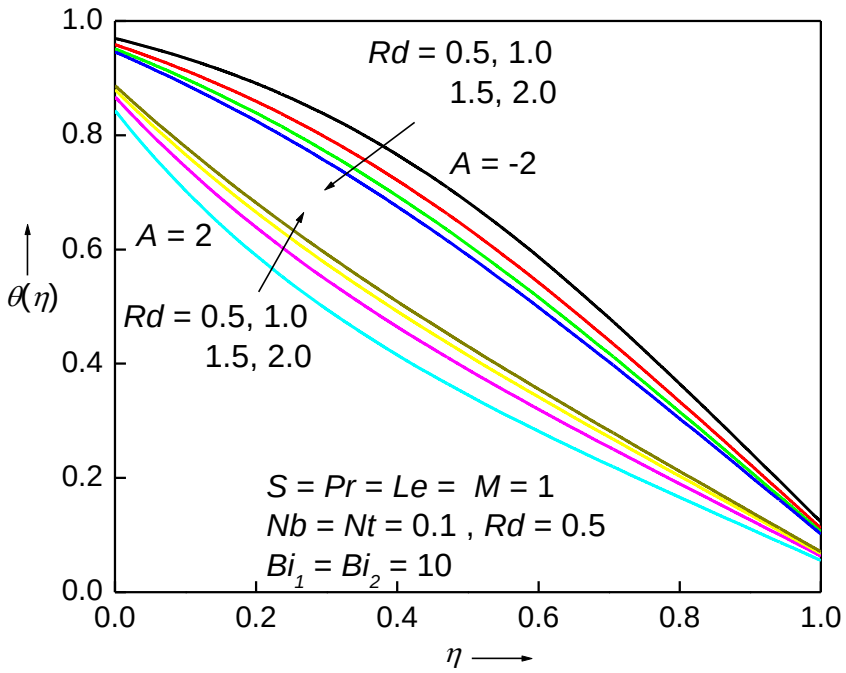

Fig 12a Influence of *Rd* on $\theta(\eta)$ for equal Biot numbers

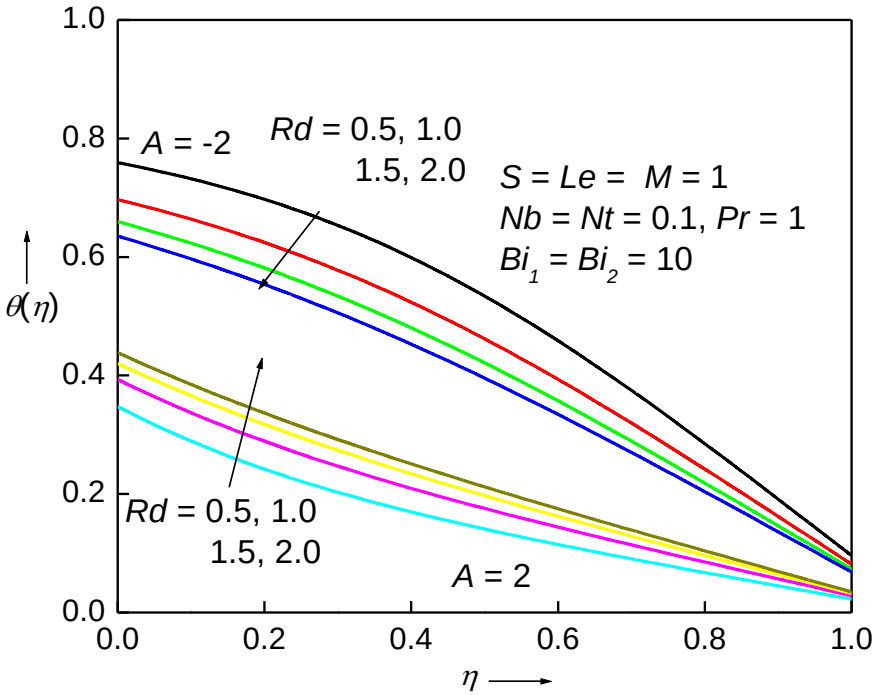

Fig 12b Influence of *Rd* on $\theta(\eta)$ for unequal Biot numbers

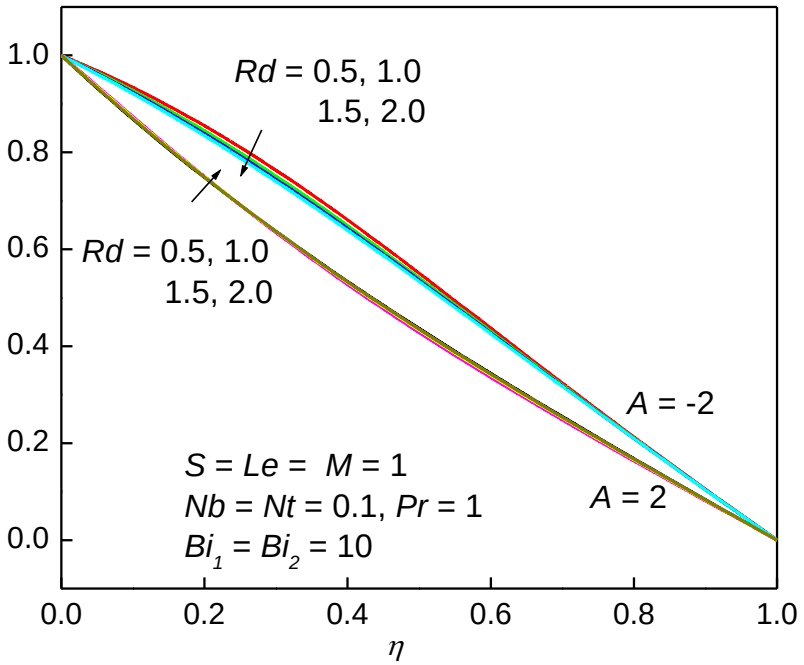

Fig 13a Influence of *Rd* on $\phi(\eta)$ for equal Biot numbers

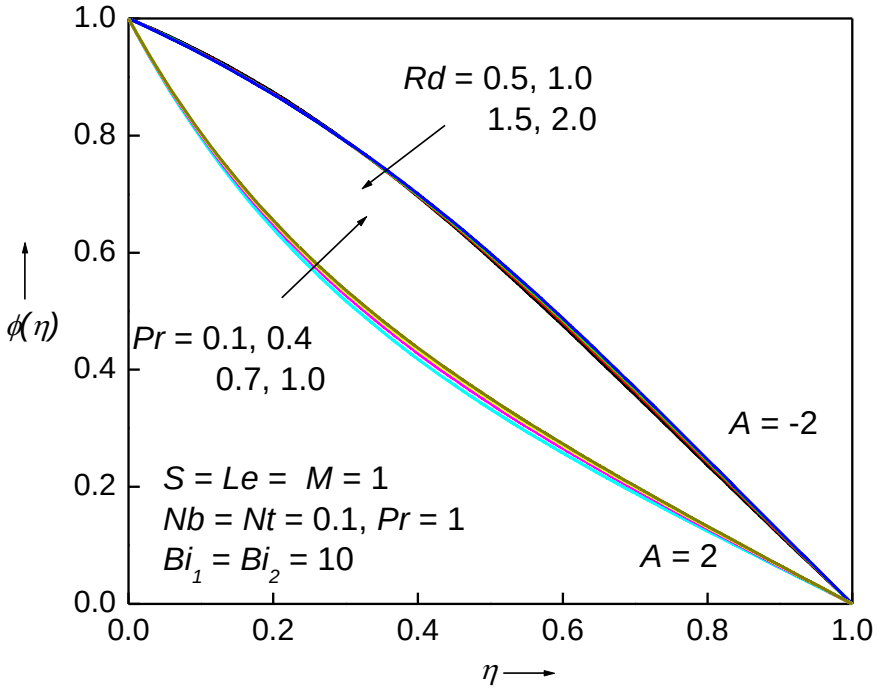

Fig 13b Influence of *Rd* on $\phi(\eta)$ for unequal Biot numbers

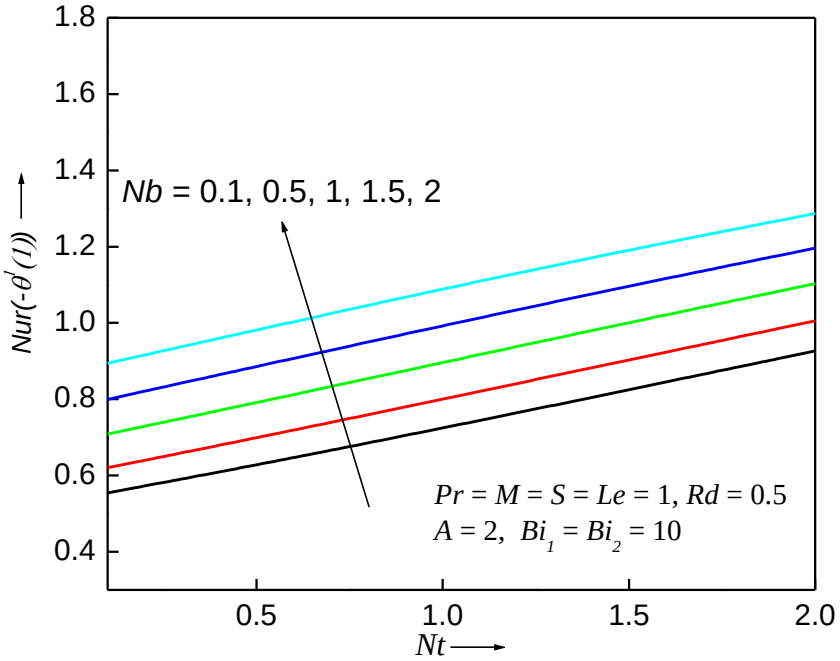

Fig. 14a. Influence of *Nb* and *Nt* on *Nur* for equal Biot numbers

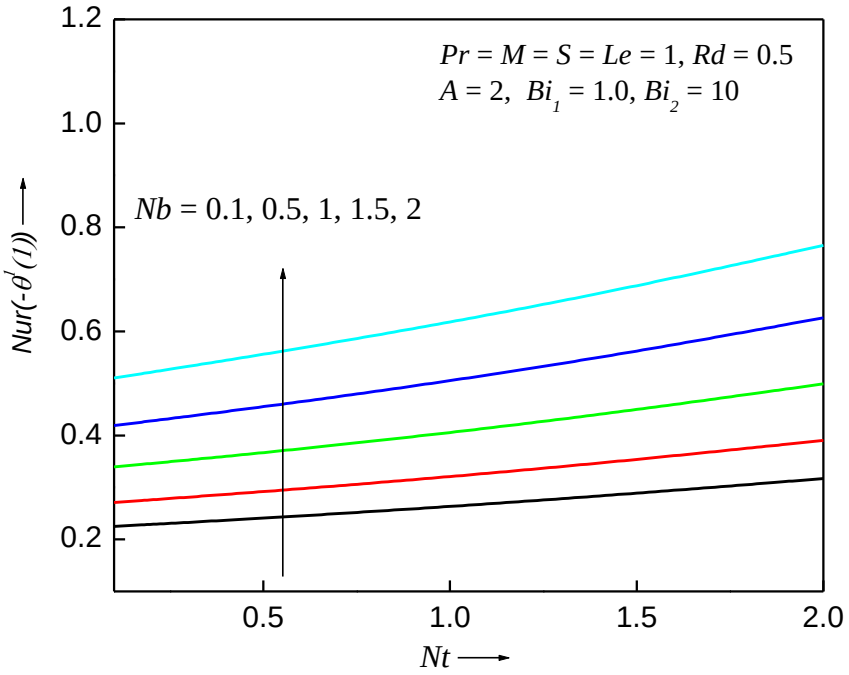

Fig. 14b. Influence of *Nb* and *Nt* on *Nur* for unequal Biot numbers

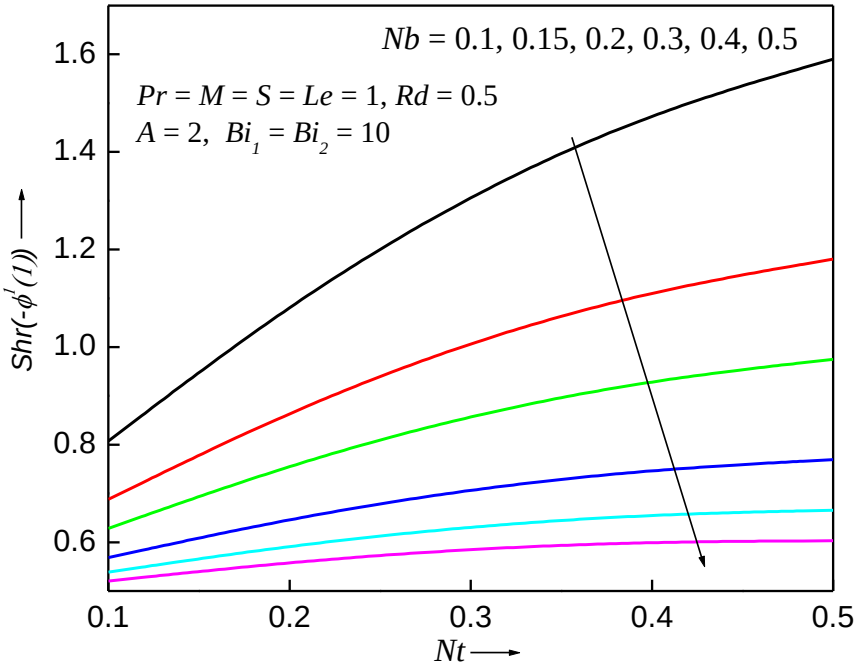

Fig. 15a. Influence of *Nb* and *Nt* on *Shr* for equal Biot numbers

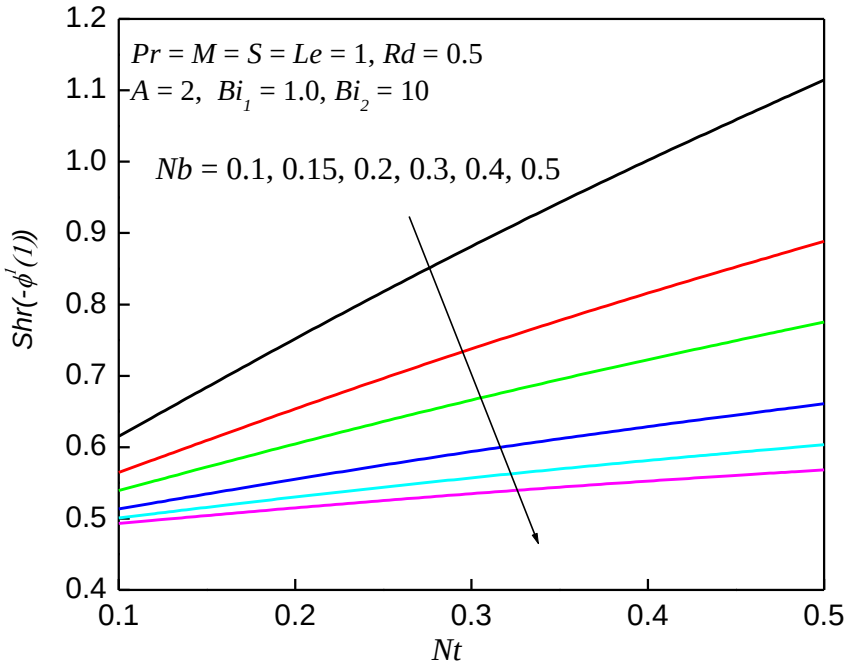

Fig. 15b. Influence of *Nb* and *Nt* on *Shr* for unequal Biot numbers

Table 1. Comparison table for Skin friction coefficient $f^{11}(1)$ for different values of M and S, $A=2, P=Le=1, Nb=Nt=0.1, Rd=0$.

M	S	$f^{11}(1)$		
		Present $Bi_1=Bi_2=10$	Present $Bi_1=1.0,\ Bi_2=10$	Reference HAM
0	1	7.53313247	7.53313247	7.53316579
2	1	8.26383886	8.26384197	8.26387231
3	1	9.09725938	9.09726618	9.09732572
5	1	11.34929888	11.34931578	11.3492890
1	0.1	8.97546290	8.97546290	8.97552394
1	0.5	8.34917873	8.34916801	8.34924578
1	1	7.72190940	7.72191376	7.72194601
1	2	6.94081636	6.94082584	6.94077326

Conclusion:

This model derived for chemically reacted radiated unsteady squeezing flow of magnetonanoliquid through the parallel disks. The main results associated with this study is listed as fallows,

- The temperature effect is directly related with N_t and N_b
- Temperature and concentration effect both are quite opposite against to squeezing parameter S
- M and Rd values rises the nanoliquid temperature.
- Skin frictions are enhanced via M and revers trend found for S.
- Rate of mass transfer at lower disk augments with S, Le and N_t.

Reference List:

Stefan M. J., Versuch Uber die scheinbare adhesion, Akademie der Wissenschaften in Wien. Mathematik-Naturwissen. 1874; 69: 713.

Kuzma D. C., Fluid inertia effects in squeeze films. Appl Sci Res. 1967; 18: 15–20.

Siddiqui A. M., Irum S., Ansari A. R., Unsteady squeezing flow of a viscous MHD fluid between parallel plates, a solution using the homotopy perturbation method. Math Model Anal. 2008; 13: 565–76.

Sweet E., Vajravelu K., Van Gorder R. A., Pop I., Analytical solution for the unsteady MHD flow of a viscous fluid between moving parallel plates. Commun Nonlinear Sci Numer Simul. 2011;16: 266–73.

Siddiqui A. M., Irum S., Ansari A. R., Unsteady squeezing flow of a viscous MHD fluid between parallel plates, M. Mod. Ana, 13, (2008) 565-576.

Domairy G., Aziz A., Approximate Approximate Analysis of MHD Squeeze Flow between Two Parallel Disks with Suction or Injection by Homotopy Perturbation Method, Mathematical Problems in Engineering, article ID/2009/603916

Joneidi A., Domairry A. G., Babaelahi M., Effect of mass transfer on the flow in the magnetohydrodynamic squeeze film between two parallel disks with one porous disk, Chem. Eng. Comm., 198, (2011) 299-311.

Hayat T., Yousuf A., Mustafa M., Asghar S., Influence of Heat Transfer in the Squeezing Flow Between Parallel Disks, Chem. Eng. Comm., 199 (2012), 1044 - 1062.

Cortell R., Chem. Eng. Res. Des. ***89****, 85 (2011).*

Pal D., Chatterjee S., Commun. Nonlinear Sci. Numer. Simulat. 15, 1843 (2010).

Badruddin I. A., Zainal Z. A., Narayana P. A. A., Seetharamu K. N., Numerical analysis of convection conduction and radiation using a non-equilibrium model in a square porous cavity, Int. J. Thermal Sciences, 46 (2007), pp. 20-29.

Badruddin I. A., Zainal Z. A., Khan Z. A., Mallick Z., Effect of viscous dissipation and radiation on natural convection in a porous medium embedded within vertical annulus, Int. J. Thermal Sciences, 46 (2007), pp. 221-227.

Ahmed S. E., Hussein A. K., Mohammed H. A., Adegun I. K., Zhang X., Kolsi L., Hasanpour A., Sivasankaran S., Viscous dissipation and radiation effects on MHD natural convection in a square enclosure filled with a porous medium, Nuclear Engineering and Design, 266 (2014), pp. 34-42.

Ahmed S. E., Oztop H. F., Al-Salem K., Natural convection coupled with radiation heat transfer in an inclined porous cavity with corner heater, Computers & Fluids, 102 (2014), 10, pp. 74-84.

Mahapatra T. R., Pal D., Mondal S., Combined effects of thermal radiation and heat generation on natural convection in a square cavity filled with Darcy-Forchheimer porous medium, Int. J. Applied Mathematics and Computation, 4 (2012), 4, pp. 359-368.

Marina S. A., Mikhail A. S., Jawali C. U., Effect of thermal radiation on natural convection in a square porous cavity filled with a fluid of temperature-dependent viscosity, Thermal Science (only online available).

Adesanya S. O., Ogunseye H.A., Jangili S., Unsteady squeezing flow of a radiative Eyring–Powell fluid channel flow with chemical reactions. Int J Therm Sci. 2018; 125: 440 - 7.

Balazadeh N., Sheikholeslami M., Ganji D. D., Li Z., Semi analytical analysis for transient Eyring–Powell squeezing flow in a stretching channel due to magnetic field using DTM. J Mol Liq. 2018; 260: 30–6.

Das K., Int. J. Heat Mass Transfer ***54****, 3505 (2011).*

Hayat T., Nawaz M., Sajid M., Asghar S., Comput. Math. Appl. ***58****, 369 (2009).*

Bhattacharyya K., Mukhopadhyay S., Layek G. C., Pop I., Int. J. Heat Mass Transfer ***55****, 2945 (2012).*

Ikram Ullah, Muhammad W., Hayat T., Ahmed Alsaedi, Khan M. I., Thermally radiated squeezed flow of magneto-nanofluid between two parallel disks with chemical reaction.

Martyushev S. G., Sheremet M. A., Characteristics of Rosseland and P-1 approximations in modeling nonstationary conditions of convection-radiation heat transfer in an enclosure with a local energy source, J. Engineering Thermophysics, 21 (2012), 2, pp. 111-118.

Kierzenka J., Shampine L. F., A BVP solver based on residual control and the Maltab PSE, ACM Transactions on Mathematical Software, 27(3) (2001) pp 299-316.

Hashmi M. M., Hayat T., Alsaedi A., On the analytic solutions for squeezing flow of nanofluid between parallel disks, Nonlinear Analysis: Modelling and Control, 17(4) (2012), pp. 418-430.